

# Time delay prediction for space telerobot system with a modified sparse multivariate linear regression method

Haifei Chen<sup>a,b</sup>, Panfeng Huang<sup>a,b,\*</sup>, Zhengxiong Liu<sup>a,b</sup>, Zhiqiang Ma<sup>a,b</sup>

<sup>a</sup> National Key Laboratory of Aerospace Flight Dynamics and Research Center for Intelligent Robotics, China

<sup>b</sup> School of Astronautics, Northwestern Polytechnical University, Xi'an, 710072, China

## ARTICLE INFO

### Keywords:

Space telerobot system (STS)  
Time delay prediction  
Modified sparse multivariate linear regressive (SMLR)

## ABSTRACT

Compared with general telerobot system, space telerobot system (STS) faces with more serious and complex time delay. In time delay prediction, the traditional sparse multivariate linear regressive (SMLR), auto regressive (AR), neural network (NN) and cubic polynomial model based (CBMB) approaches share lower efficiency or precision, when time delay is serious and complex. To solve this problem, time delay prediction for STS is discussed in this paper. Through analysis, time delay in STS can be divided to three parts: a) communication time delay; b) transmission time delay; c) processing time delay. Then, detailed varying rule and accurate statistics analysis are given for each parts of time delay. Based on the previous work, a modified SMLR is proposed and realizes the prediction of time delay. Compared with previous SMLR, AR, NN and CBMB approaches, the modified SMLR method shares more higher prediction efficiency or precision. Finally, a simulation example is given and the simulation results show the superiorities.

## 1. Introduction

Typical space telerobot system (STS) is given as Fig. 1 and composed of ground control-center, ground base station, communication channel, space base-station and operation target [1]. STS is a representative human-machine collaboration system [2]. It makes full use of the capacity that robot accomplishes the remote task. Meanwhile, human intelligence is integrated to it, to execute complex mission or dispose accident. Hence, it shares good prospects and is the hot issue in robotics.

Time delay is the biggest obstacle in improving properties for all telerobot systems [3]. However, besides huge communication (transmission) delay, STS also faces with complex disposing time delay. Furthermore, processing time delay always is dominant in the round trip time delay (RTTD) of STS [4]. As a result, comparing with the general telerobot system, STS faces more serious and complex time delay. By analyzing Fig. 1, RTTD of STS is made up of three parts: a) communication time delay between the ground base-station and control-center; b) transmission time delay between the ground and space base-stations; c) processing time delay generating from the ground control-center, ground and space base-stations.

For time delay problem, many approaches have applied to the general telerobot systems, like passive-based control [5–7], robust

control [8–14], impedance control [15–19] and predictive control methods [20–27] and so on. With further disposal, all of those methods can be extended to the STS. However, only predictive control method can simultaneously improve stability and transparency, especially the predictive display control method. All of the others make compromise between stability and transparency, as they, more or less, directly use the delayed information as control signal [28]. In predictive display control method, the visual and tactile information can be perceived synchronously and simultaneously [29]. Hence, predictive display control enhances the telepresence deeply. As a result, it may be the most valuable and prominent control approach for STS.

In predictive display control method, one of the core problems is predictor design. As [28] stated, the predictor structure can be divided into three kinds: Smith predictor (SP), model-based predictor and model/generalized predictive control. In SP structure, it only needs to know the RTTD, where RTTD is comprised of forward and backward time delays. In the other two predictor structures, the forward and backward time delays should be provided. However, in practical STS, time delay measuring is often in the form of RTTD. Hence, the SP structure is utilized in this paper [28].

Because SP structure requires RTTD is known in advance, it implies time delay prediction is necessary. For time delay prediction, many previous works referred to the general telerobot system [30–37], but

\* Corresponding author. National Key Laboratory of Aerospace Flight Dynamics and Research Center for Intelligent Robotics, China.

E-mail addresses: chenzhouchf@mail.nwpu.edu.cn (H. Chen), phuang@nwpu.edu.cn (P. Huang), liuzhengxiong@nwpu.edu.cn (Z. Liu), zhiqiangma@nwpu.edu.cn (Z. Ma).

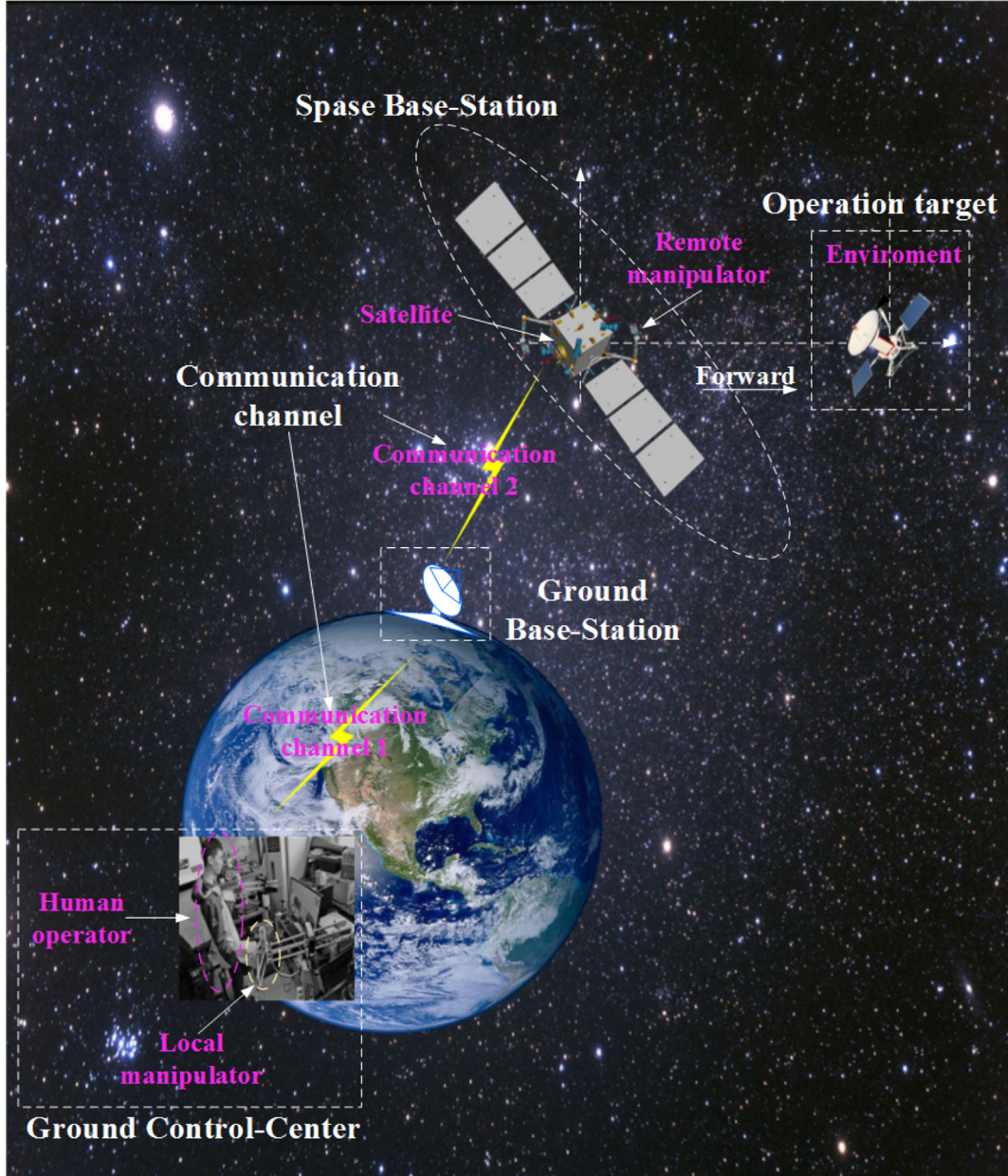


Fig. 1. Typical space telerobot system (STS).

not STS. Moreover, only the Internet network communication delay is considered. Thus, it's meaningful to study the time delay prediction in STS or extend the previous results to STS. However, the neural network (NN), auto regressive (AR) and sparse multivariate linear regressive (SMLR) prediction methods referred in the aforesaid papers are not suitable for STS. The reasons are that time delay exists violent jitters or prediction efficiency decreases with the time goes by. Moreover, RTTD of STS is composed by three parts and different parts have different varying rules and statistical characteristics. Hence, single method simultaneously predicts those three parts is difficult, as illustrated in Ref. [4]. However, time delay measuring in STS is often in the form of RTTD, as stated before. Thus, it's meaningful and helpful to predict all those three parts time delay with single method.

Previous analysis motivate us to make this study. In this paper, by analyzing the communication structures or information loops, varying rules of each parts time delay are obtained. Meanwhile, accurate statistics analysis are conducted, with histogram, phase plot and auto-correlation tools. Then, a modified SMLR method is proposed, basing on

the previous works. With the proposed method, prediction of the time delay in STS is realized. Subsequently, a Smith predictive control structure is designed to ensure the system stability. Meanwhile, the force feedback in local side and position tracking in remote side are guaranteed. Finally, superiorities of the modified SMLR method is illustrated by a simulation example. In the simulation example, comparisons between the modified SMLR, traditional SMLR, NN, AR and cubic polynomial model based (CBMB) methods are given.

Main contributions of this paper are given as follows:

- 1) Detailed analysis about the varying rules and statistical characteristics of each parts time delay in STS are given. Following those work, choosing of time delay prediction method will be more directional and reasonable;
- 2) A modified SMLR method is proposed, featuring with high prediction efficiency and accuracy. Based on this method, the prediction of all three parts time delay in STS is realized.

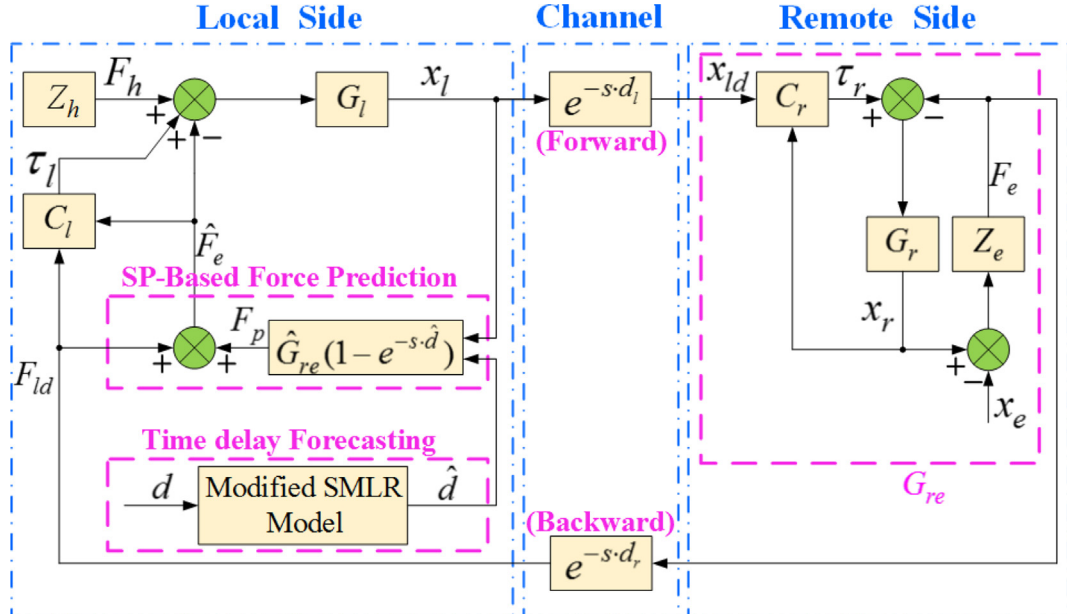


Fig. 2. Closed-loop STS control structure.

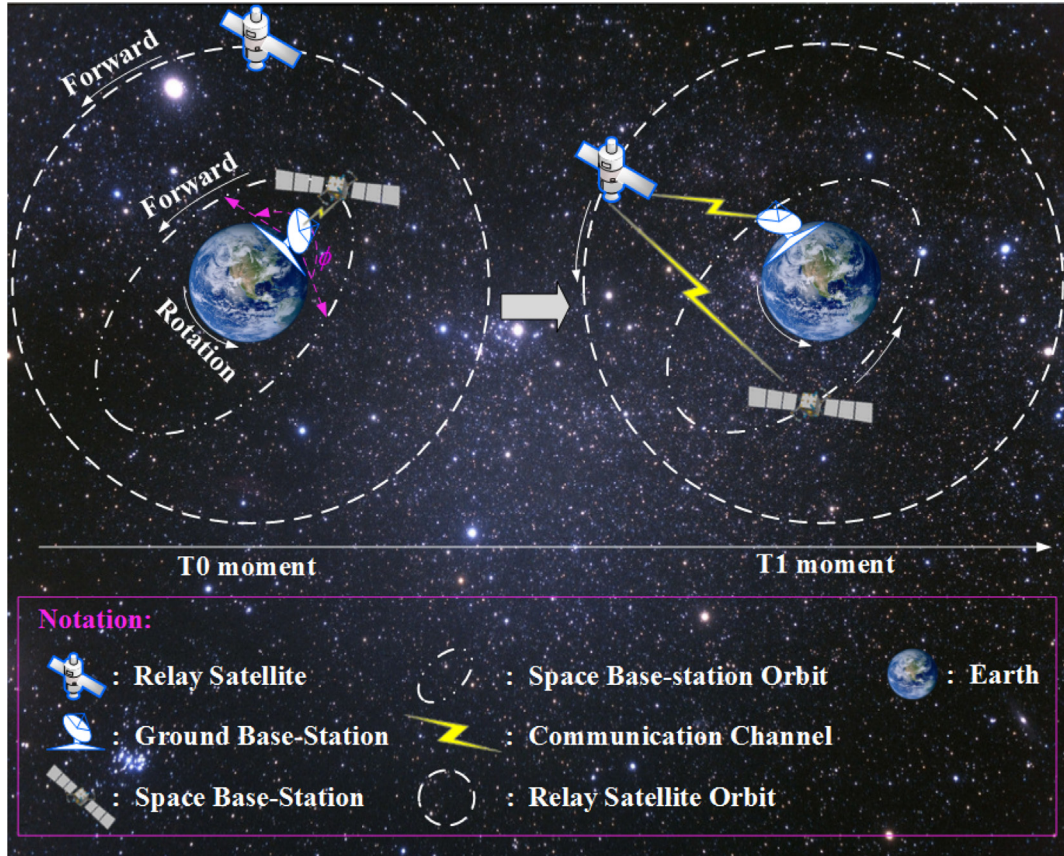


Fig. 3. Topological structure of “Communication channel 2”.

Structure of this paper: In section 2, preliminaries concerning STS dynamics and control structure are given first. Then, time delay varying rules are discussed. In section 3, time delay statistical characteristics analysis, time delay prediction and system stability analysis are illustrated. Section 4 and 5 are the simulation and conclusion, respectively.

## 2. Preliminaries

In this section, STS dynamics and control structure are illustrated first, where Smith predictor work mechanism also are explained. Then, preliminary analysis of time delay varying rules are given.

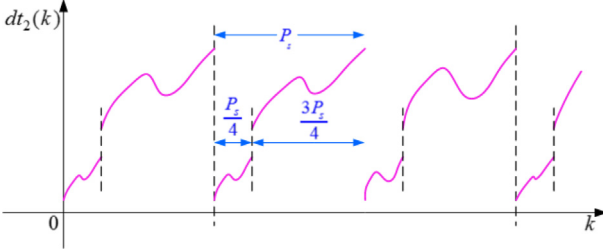


Fig. 4. The varying curve of  $dt_2(k)$ .

## 2.1. Preliminaries concerning STS dynamics/structure

The control structure of STS is showed in Fig. 2. The corresponding relationships between the modules in Fig. 1 and notations in Fig. 2 are given as follows: 1)  $Z_h$  and  $G_l$  are human operator and local manipulator,<sup>1</sup> respectively; 2)  $Z_e$  and  $G_r$  are the environment and remote manipulator, respectively. In addition,  $C_l$  and  $C_r$  represent the local and remote controllers, respectively.  $G_{re}$  is the model of environment + remote manipulator and  $\hat{G}_{re}$  is the estimation model of  $G_{re}$ . Forward and backward time delays are  $d_l$  and  $d_r$ , respectively.  $d = d_l + d_r$  is the RTTD and  $\hat{d}$  is the prediction value of  $d$ .

To simplify the analysis, the local and remote manipulator models  $G_l$  and  $G_r$  are chosen as the linear form in this paper. It is given in time domain as follows:

$$\begin{aligned} M_l \ddot{q}_l + H_l \dot{q}_l &= \tau_l + F_h - \hat{F}_e \\ M_r \ddot{q}_r + H_r \dot{q}_r &= \tau_r - F_e \end{aligned} \quad (1)$$

where the subscript  $i = l/r$  represents the local and remote manipulators, respectively.  $q_i \in R^n$ ,  $\dot{q}_i \in R^n$  and  $\ddot{q}_i \in R^n$  denote the joint position, velocity and acceleration, respectively.  $M_i \in R^{n \times n}$  is the positive-definite inertia matrix.  $H_i \in R^{n \times n}$  is the matrix of centripetal and coriolis torque.  $\tau_i \in R^n$  is the applied control torque, generating from the controller  $C_i$ .  $F_h \in R^n$  and  $F_e \in R^n$  are the human operator and environment forces, respectively. Moreover,  $M_i$  and  $H_i$  are constant matrices or vectors.

Prediction reflected force  $\hat{F}_e$  is generated from the “SP-Based Force Prediction” unit in Fig. 2. It is given as

$$\hat{F}_e = \hat{G}_{re}(1 - e^{-sd})x_l + F_{ld} \quad (2)$$

where  $F_{ld} = e^{-sd}G_{re}x_l$  can be deduced from Fig. 2. Hence, if  $\hat{G}_{re} = G_{re}$  and  $\hat{d} = d$  hold,  $\hat{F}_e$  becomes  $\hat{F}_e = G_{re}x_l$ , which implies perfect elimination of the time delay influences. As  $G_{re}$  is assumed definite and known in advance, there exists  $G_{re} = \hat{G}_{re}$  in this paper. Thus, the prediction precision of the  $\hat{F}_e$  is only related to  $\hat{d}$ . In summary, the force synchronization  $F_h = \hat{F}_e e^{-sd}$  in the local side will be guaranteed, only if the time delay prediction precision is good enough. Additionally, human operator shares good compensation capability of dynamic torque, which implies that  $\hat{F}_e = F_h$  and the human operator can perceive the prediction force  $\hat{F}_e$ , directly.

Thus, from a control standpoint, only the remote side position synchronization  $x_r = x_l e^{-sd}$  will be considered and the master side will be not deeply discussed in the rest of this paper. Moreover, assuming the local side of STS is stable, which implies force synchronization error  $F_h - F_e(t - d_r)$  and states  $q_l$ ,  $\dot{q}_l$  and  $\ddot{q}_l$  are bounded.

Let the state variable of the remote manipulator as  $x_r = [q_r^T, \dot{q}_r^T]^T$ . Then, (1) can be rewrote as:

$$\dot{x}_r = A_r \cdot x_r + B_r \cdot (\omega_r + M_r^{-1} \tau_r) \quad (3)$$

<sup>1</sup>The local and remote manipulators are often called master and slave. However, in bilateral teleoperation the slave influences the master, and it can move according to the slave. Hence, it would be better to call them local and remote robot manipulators or, simply, local and remote [39].

where  $A_r = [0_{n \times n}, I_{n \times n}; A_{21}, A_{22}]$ ,  $B_r = [0_{n \times n}; I_{n \times n}]$ ,  $\omega_r = -M_r^{-1}(H_r \dot{q}_r + F_e) - [A_{21}, A_{22}]x_r$ .  $A_{21}$  and  $A_{22}$  are negative-definite diagonal matrices.

In this paper,  $\tau_r$  is designed as follows:

$$\tau_r = -M_r \cdot \omega_r + M_r \cdot u_r \quad (4)$$

where  $u_r = -[A_{21}, 0_{n \times n}] \cdot x_{ld} + \dot{q}_{ld} - \dot{q}_{ld} - q_{ld}$  and  $x_{ld} = x_l(t - d_l) = [q_l^T(t - d_l), \dot{q}_l^T(t - d_l)]^T$ . Hence, (3) can be rewrote as

$$\dot{x}_r = A_r \cdot x_r + B_r \cdot u_r \quad (5)$$

## 2.2. Preliminary analysis of time delay varying rules

As Fig. 1 illustrated, RTTD of STS is composed of three parts: 1) communication time delay  $dt_1$ , generating from “Communication channel 1”; 2) transmission time delay  $dt_2$ , generating from “Communication channel 2”; 3) processing time delay  $dt_3$ , generating from ground control center, ground and space base-stations.

According to Refs. [4,30,32,37],  $dt_1$  complies with shifted Gamma distribution. However, there still exists a controversy that  $dt_1$  satisfies the short or long range autocorrelations, as long range autocorrelation is considered in Ref. [30] and short range autocorrelation is obtained in Ref. [30]. In fact,  $dt_1$  actually obeys the short range autocorrelation in a short period, but with a long range autocorrelation in the averages during different periods. Illustrations about this fact are given in Fig. 6, basing on statistics analysis.

For  $dt_2$ , “Communication channel 2” of Fig. 1 is the source of it. As is well known, space base-station can't often communicate with the ground base-station all the time. As a result, operation time segment for operating space robot is limited or even very short in a day. To help understand limited operation time segment, Fig. 3 is given with a detailed description of the “Ground base-station, Communication channel 2 and Space base-station” in Fig. 1. Additionally, relay satellites also are included for solving the communication interruption between the ground and space base-stations, more details referred to Fig. 3.

In Fig. 3, the left and right sides give the positions of STS at time T0 and T1, respectively, where  $T0 < T1$ . At T0, the ground and space base-stations locate at the same side of the earth and they can communicate directly with each other. However, there often exists a fact that the ground and space base-stations are not relative rest. Hence, the ground and space base-stations may move to different sides of the earth, as moment T1 illustrated. Obviously, the communication between the ground and space base-stations is break down at T1. Then, remedial measures are needed to maintain the continuous communication between them. Thus, a relay satellite with locating at geosynchronous orbit is added to the STS, which is relative rest with the earth and ground base-station. Under this case, the relay satellite acts as the rule of signal relay. Hence, besides the direct communication topological structure (the space base-station communicates directly with the ground base-station), a relay communication topological structure (the space base-station communicates with the ground base-station through relay satellite) for “Communication channel 2” appears.

As a result, “Communication channel 2” in Fig. 1 switches between two kinds of communication topology structure. With this switching mechanism, continuous teleoperation is realized. Before further disposal, the space base-station revolution period is given first, as  $P_s = 1.659 \times 10^{-4}(R_e + h)^{\frac{3}{2}}$ . In  $P_s$ , the earth radius  $R_e \approx 6378$  km and  $h$  is the average height of the space base-station.

Hence, the time of “Communication channel 2” utilizing the direct communication structure is about  $\frac{P_s}{4}$  in a revolution period  $P_s$ , with sweeping the angle  $\varphi$ . Then, the relay communication structure is about  $\frac{3P_s}{4}$  with sweeping the angle  $2\pi - \varphi$ . Based on the analysis of Fig. 3, varying rule of  $dt_2$  is approximate to a cubic polynomial curve (as Fig. 4), whatever the “Communication channel 2” uses the direct and relay communication structures.

Data processing in STS mainly appears in the ground control-center,

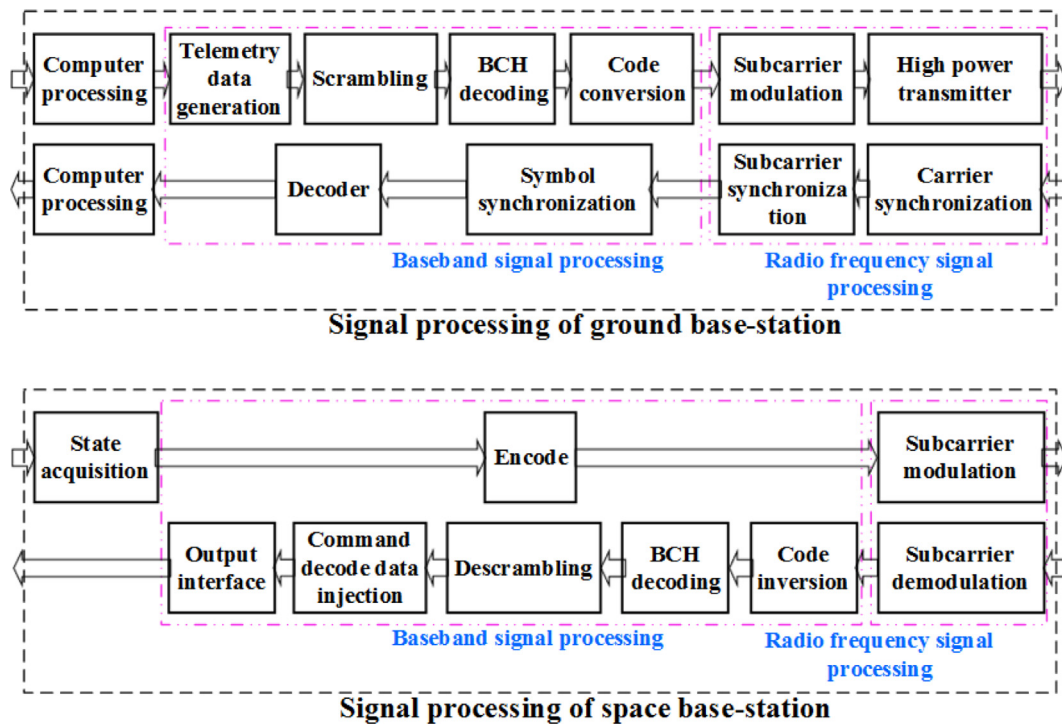
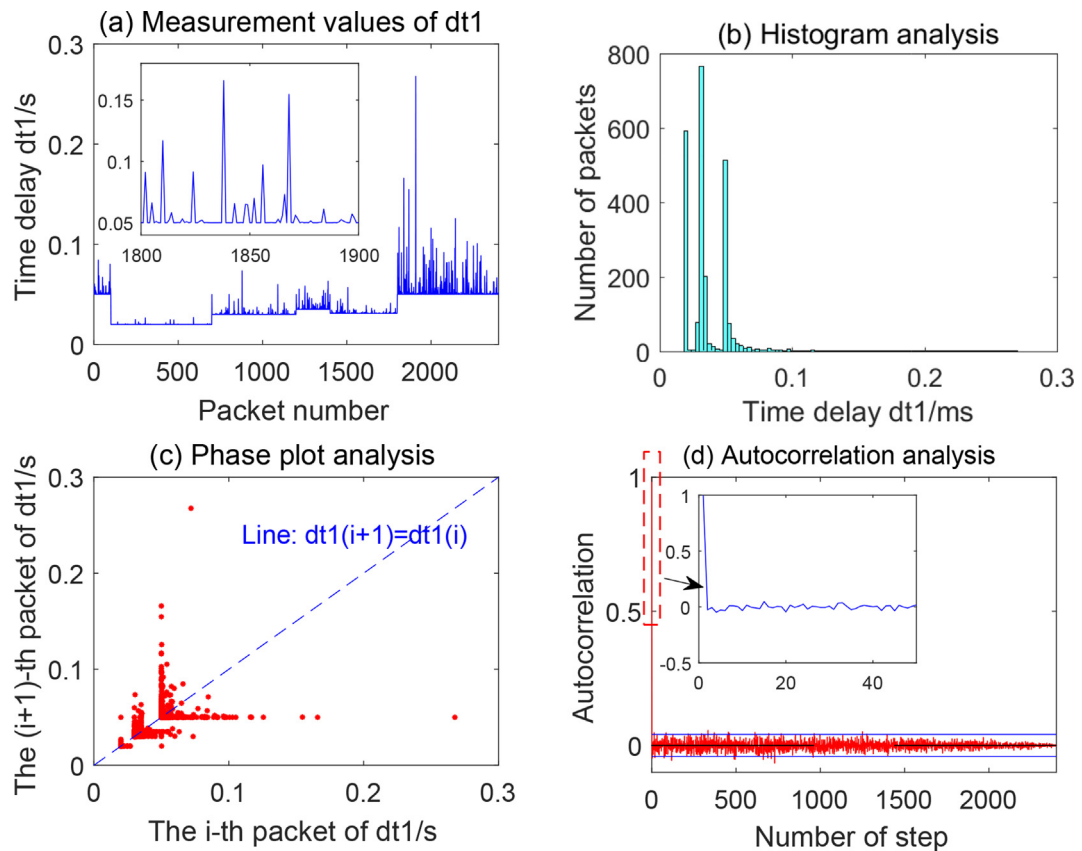
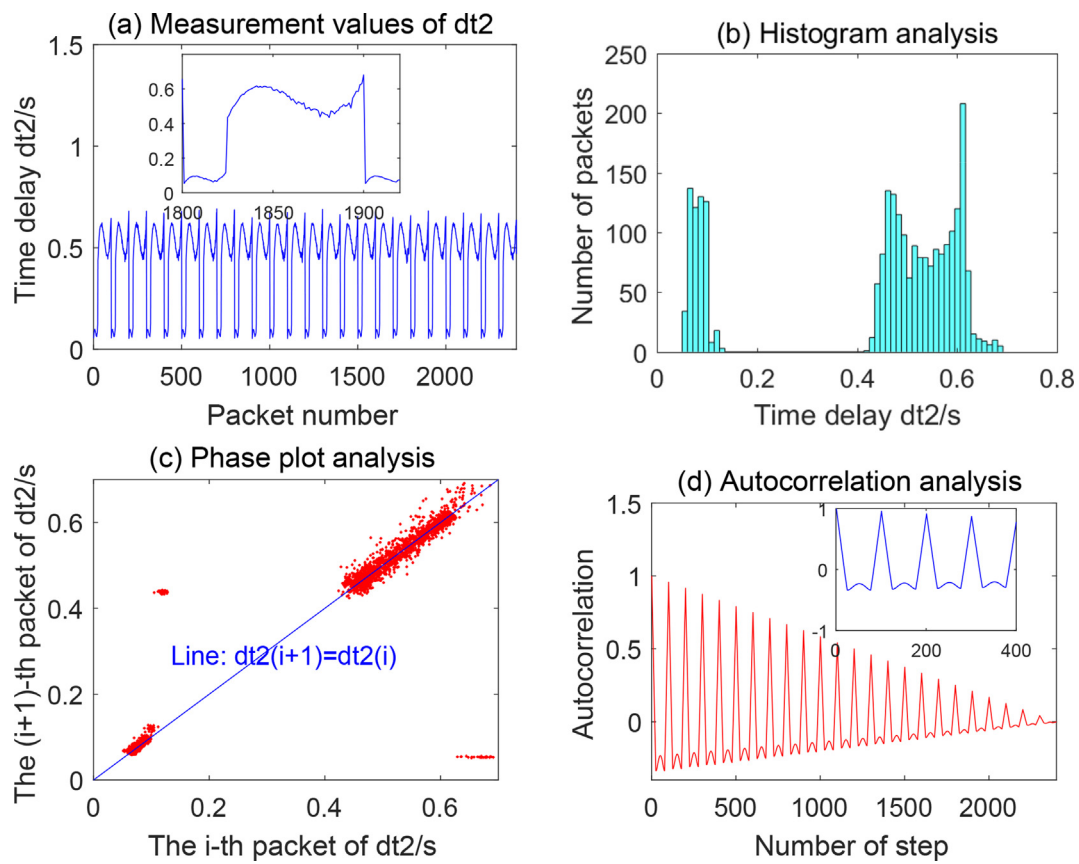
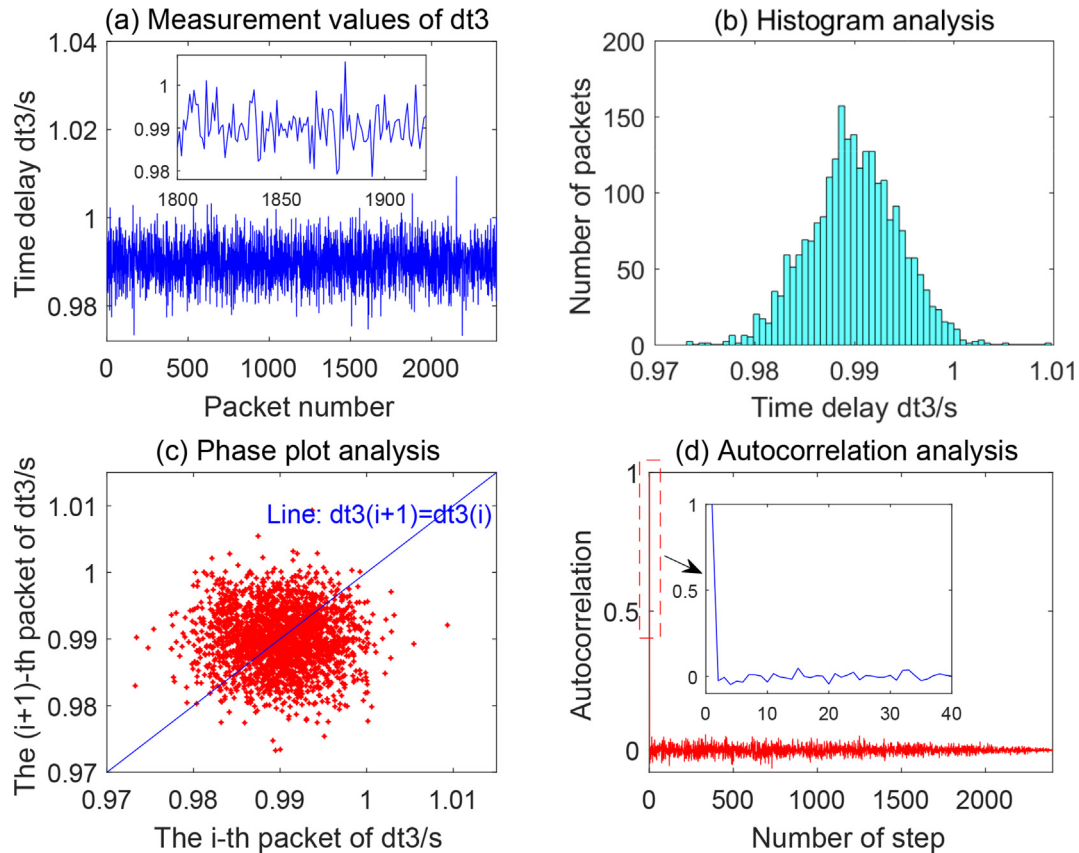


Fig. 5. Data processes of the ground control-center, ground and space base-stations.

Fig. 6. Statistics characters analysis of  $dt_1$ .

ground and space base-stations. The detailed disposal processes of the ground and space base-stations are given in Fig. 5, which is the base of modeling the third part time delay in STS. In Fig. 5, there are so many processing steps and complex information loops. Hence, this part of

time delay always is the most serious one, comparing with the other two parts in STS. With the analysis of Fig. 5 and previous work in Ref. [4], the processing time delay  $dt_3$  in STS approximately obeys the normal distribution. Additionally, varying range of  $dt_3$  is relatively smooth and

Fig. 7. Statistics characters analysis of  $dt_2$ .Fig. 8. Statistics characters analysis of  $dt_3$ .

**Table 1**  
Statistics characters of  $dt_1$ .

Character	$dt_1$
Probability distribution	Shifted Gamma distribution
Change rule	Random variation
Autocorrelation	Short-range autocorrelation

**Table 2**  
Statistics characters of  $dt_2$ .

Character	$dt_2$
Probability distribution	Unknown or no obvious characteristic
Change rule	Periodic variation
Autocorrelation	Short-range autocorrelation

**Table 3**  
Statistics characters of  $dt_3$ .

Character	$dt_3$
Probability distribution	Normal distribution
Change rule	Random variation
Autocorrelation	Short-range autocorrelation

steady.

### 3. Main results

In this section, time delay statistics analysis results are given first. Then, based on the statistics and varying rules analysis results, the time delay prediction method is proposed. Finally, the stability analysis results of STS are illustrated in the final of this section.

#### 3.1. Time delay statistical characteristics analysis

Following as [4,30,38], histogram, phase plot and autocorrelation are utilized to study the statistical characteristics of time delay. As stated in Ref. [4]: 1) histogram has a closed relationship with the probability density distribution; 2) phase plot shows the one-step autocorrelation property and can reflect the working load of the entire system in some sense; 3) autocorrelation shows the relationship between the present and past values. Figs. 6–8 show the statistics analysis results of  $dt_1$ ,  $dt_2$  and  $dt_3$ , respectively.

In Fig. 6, subgraph (a) is the real value of  $dt_1$ . Compared with  $dt_2$  and  $dt_3$ , this part of time delay is the most smaller one. Subgraph (b) illustrates that probability distribution of  $dt_1$  is approximated to the shifted Gamma distribution. Meanwhile, it can be imitated by three shifted Gamma distributions, according to the numbers of the peaks. Subgraph (c) shows that the points disperse around the line  $dt_1(i+1) = dt_1(i)$ . Thus, the network communication is congested or lower congested. Meanwhile, this feature of subgraph (c) also implies  $dt_1$  is random. In subgraph (d), a sharp peak can be seen, which further indicates the randomness of  $dt_1$ . However, a short-range autocorrelation can also be seen after enlarging the peak of subgraph (d). Based on the previous analysis, the statistics characters of  $dt_1$  can be summarised as follows:

In Fig. 7, subgraph (a) is the real value of  $dt_2$ . For the introduction of relay satellite, “Communication channel 2” switches periodically between the direct and relay communication modes. Thus, huge jump in switch points and periodic change character appear in  $dt_2$ . However,  $dt_2$  varies in line with a cubic polynomial changing rule, whatever the direct and relay communication modes are utilized. In subgraph (b), probability distribution of  $dt_2$  is fail to show a familiar probability distribution model. Hence, probability distribution of  $dt_2$  is unknown, based on the obtained knowledge. Subgraph (c) shows that the points

#### Modified SMLR model method:

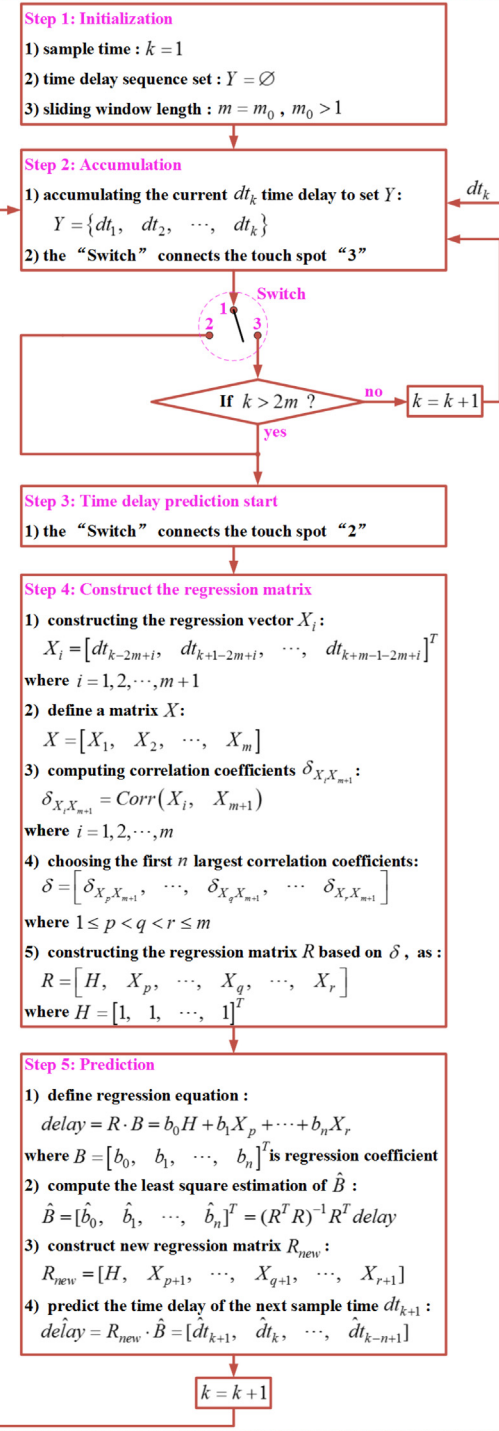
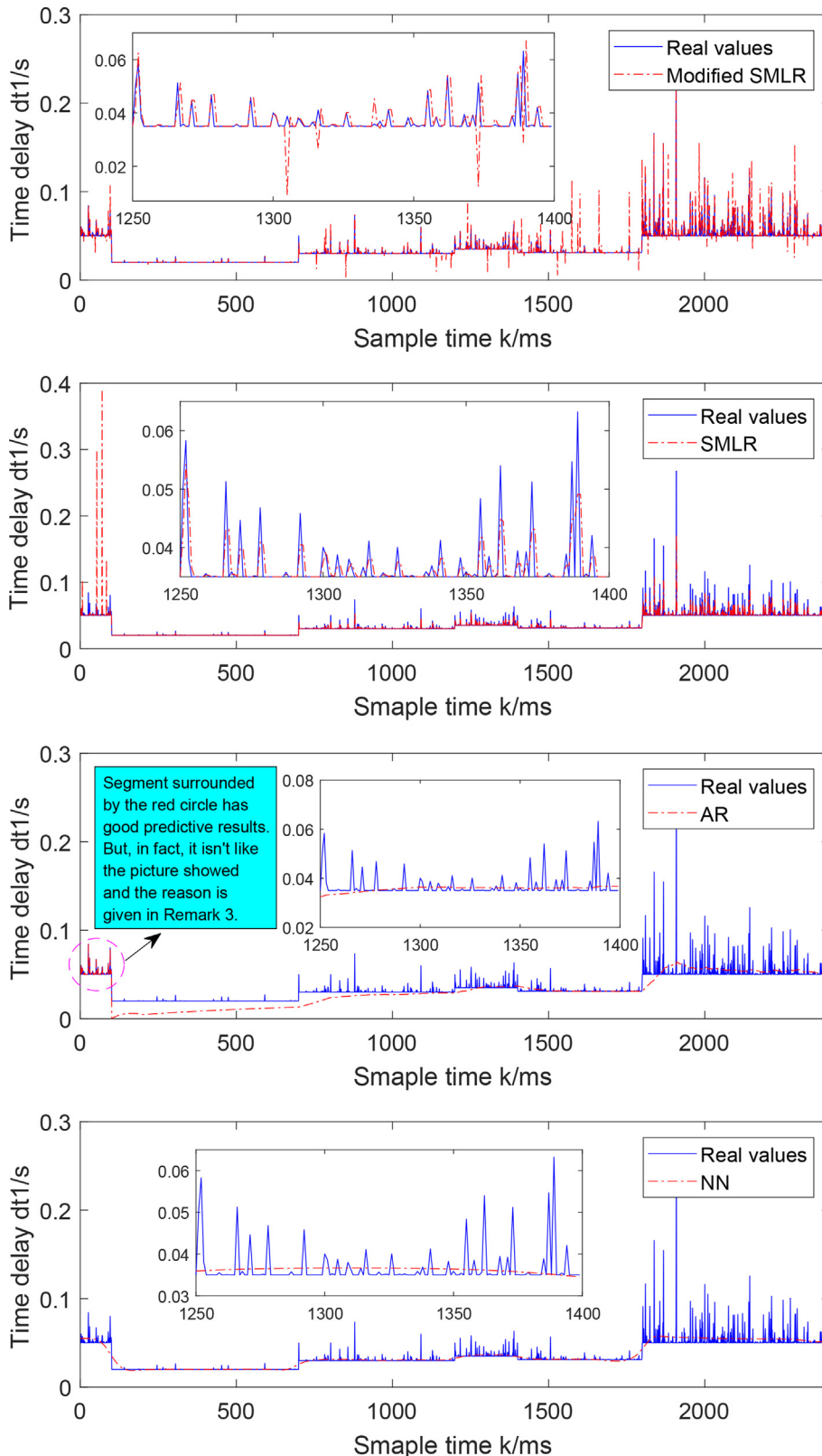


Fig. 9. Modified SMLR model method.

cluster around the line  $dt_2(i+1) = dt_2(i)$ , which implies that network communication is non-congested. Furthermore, points in subgraph (c) centralize in the line  $dt_2(i+1) = dt_2(i)$ , which is because of the short-term stabilization in  $dt_2$ . Also, the points in subgraph (c) locate on the two endpoints of the line  $dt_2(i+1) = dt_2(i)$ , which shows  $dt_2$  exists huge periodic jumps in changing process. In subgraph (d), more than one sharp peak is close to 1 in the value, which implies  $dt_2$  is not randomly varying. Moreover, after enlarging those sharp peaks in subgraph (d), short autocorrelation property can be obtained for  $dt_2$ . Based on the previous analysis, the statistics characters of  $dt_2$  can be summarised as

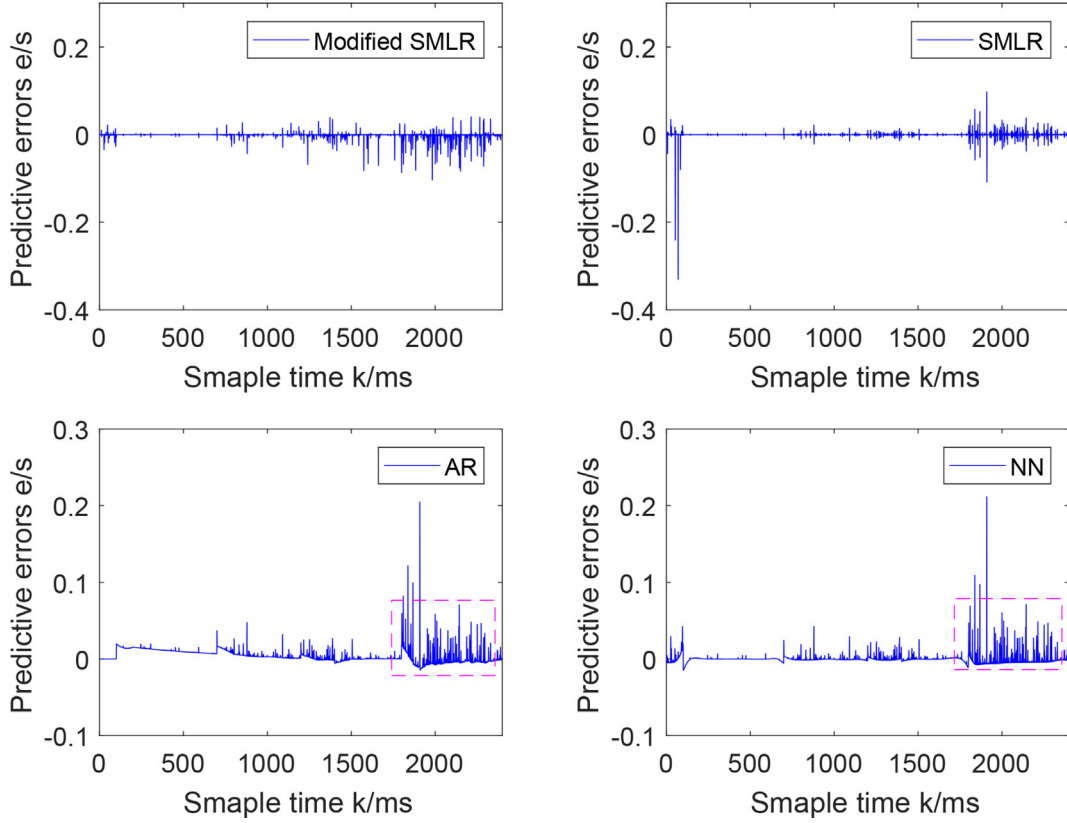


**Fig. 10.** Prediction results about time delay  $dt_1$ .

follows:

In Fig. 8, subgraph (a) is the real value of  $dt_3$ . Comparing with  $dt_1$  and  $dt_2$ , this part of time delay is often the most serious one, especially in the low-orbit STS. As illustrated in subgraph (a),  $dt_3$  shares smaller variation-range in the values, about  $990 \pm 20ms$ . According to subgraph (b),  $dt_3$  is approximate to obey the normal distribution. Similar as  $dt_1$ ,

the points in subgraph (c) disperse around the line  $dt_3(i+1) = dt_3(i)$ , which implies that the data processing procedures are congestion or lower congestion, and also indicates  $dt_3$  is random. Similarly, subgraph (4) shows  $dt_3$  features with short-range autocorrelation. Based on the previous analysis, the statistics characters of  $dt_3$  can be summarised as follows (see Tables 1–3):

Fig. 11. Prediction errors about time delay  $d_1$ .

**Remark 1.** As stated in Ref. [4], “Communication channel 1” in Fig. 1 always is based on the private network in STS. For private network, the bandwidth can be assured and network load also is determinate. Hence, compared with the general telerobot system,  $d_1$  often is more simple and with no congestion in STS. Meanwhile, only a peak will appear in the subgraph (b) of Fig. 6 in practical STS. However, in this paper, there are three peaks in subgraph (b) of Fig. 6. This is because we use the ordinary Internet network replacing the private network. As we all known, the private network is a special and simple case of the ordinary Internet network. Hence, if the case in general telerobot system can be disposed, the case in STS also can be solved. Then, the effectiveness of our methods can be further proved by making this replacement.

### 3.2. Time delay prediction

According statistics analysis illustrated before,  $d_1$  and  $d_3$  varies randomly with short-range autocorrelation property. For  $d_2$ , it changes in line with a periodic cubic polynomial curve. Then, based on the aforementioned works, a modified SMLR method is proposed to predict the RTTD in STS. Now, the modified SMLR method is given as Fig. 9.

**Remark 2.** Compared with the traditional SMLR in Ref. [30], the modified SMLR approach mainly changes in 1), 2), 3) and 4) of Step 4. In Ref. [30], the computation burden of correlation coefficients will increase with the time goes by, as the dimension of  $Y$  is increasing all the time. But in this paper, number of correlation coefficient needed to compute will be no more than  $m$ , as the existence of 3) in Step 4. Hence, the prediction efficiency can be guaranteed. Furthermore, based on the previous analysis, RTTD (including  $d_1$ ,  $d_2$  and  $d_3$ ) shares the short-range correlation property. Obviously, prediction of  $d_{k+1}$  is more relied on the adjacent past data in  $Y$ . Thus, it is reasonable to make this modification because the processing efficiency can be ensured. Also, the simulation results in section 4 illustrate the rationality. Furthermore,

superiority in prediction precision of this modified SMLR also are showed in section 4, by comparing with AR, NN-based and CPMB approaches. Especially, the modified SMLR is effective in predicting the time delay featuring with sharply jitters.

### 3.3. Stability analysis

In this section, stability analysis about the remote side of STS are given. At first, constructing a Lyapunov function as

$$V = -\frac{1}{2}e_r^T A_{21}e_r - \frac{1}{2}\dot{e}_r^T A_{21}\dot{e}_r \quad (6)$$

where  $e_r = q_l(t - d_l) - q_r$  is the position synchronization errors in remote side.

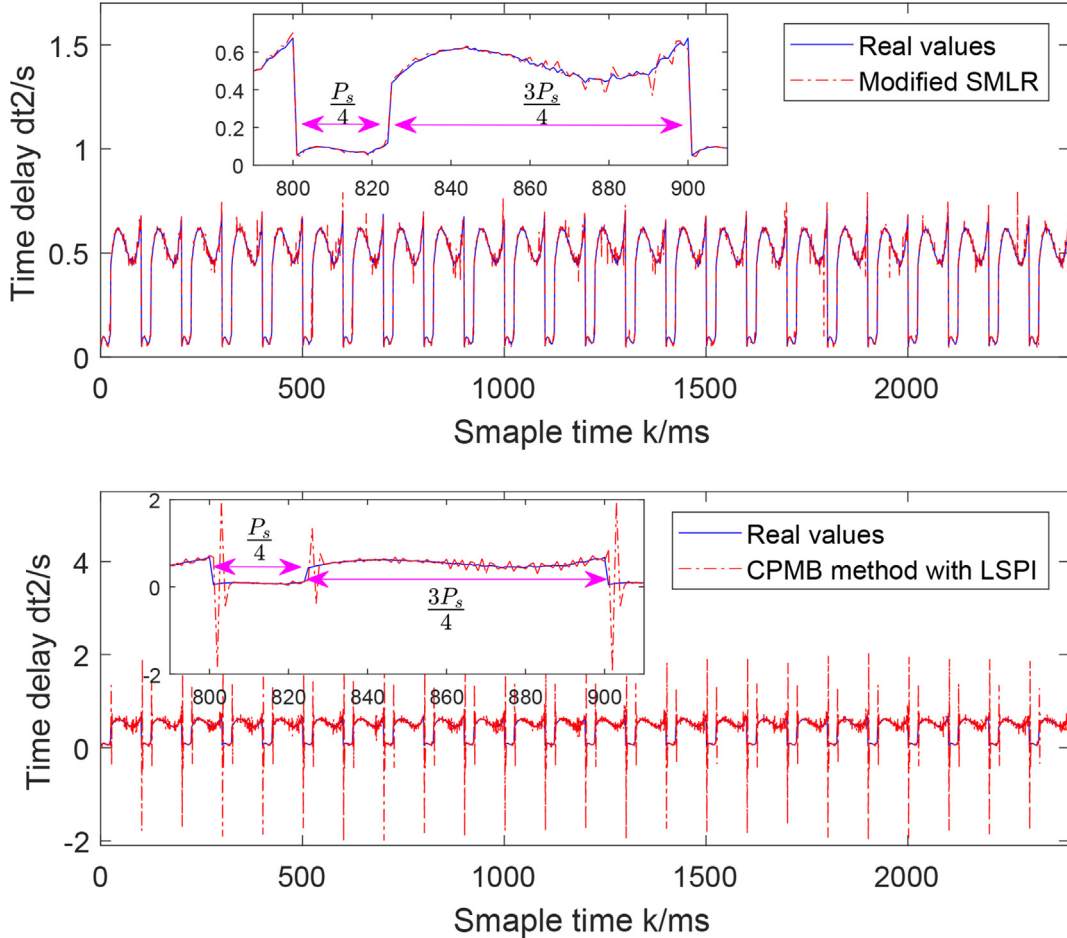
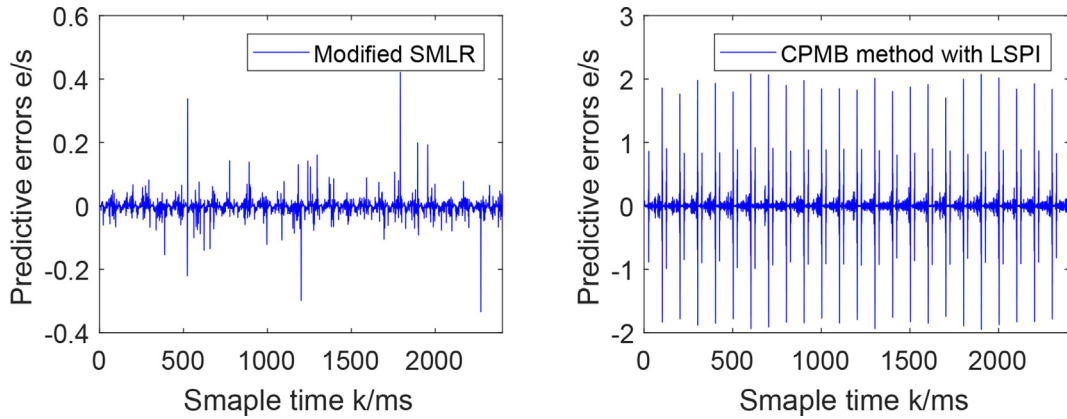
As stated before, we assume the  $q_l(t - d_l)$  and  $\dot{q}_l(t - d_l)$  are bounded. If the  $e_r$  is bounded, then the  $\dot{e}_r$  is bounded. Thus, term  $\frac{1}{2}q_r^T q_r$  is no need to appear in (6).

For  $A_{21}$  is a negative-definite diagonal matrix,  $V > 0$  holds for all the  $e_r \neq 0$  and  $\dot{e}_r \neq 0$ .

Differentiating (6) yields

$$\begin{aligned} \dot{V} &= -e_r^T A_{21} \dot{e}_r - \dot{e}_r^T A_{21} \ddot{e}_r \\ &= -[q_l(t - d_l) - q_r]^T A_{21} [\dot{q}_l(t - d_l) - \dot{q}_r] \\ &\quad - [\dot{q}_l(t - d_l) - \dot{q}_r]^T A_{21} [\ddot{q}_l(t - d_l) - \ddot{q}_r] \\ &= -[q_l(t - d_l) - q_r]^T A_{21} [\dot{q}_l(t - d_l) - \dot{q}_r] \\ &\quad - [\dot{q}_l(t - d_l) - \dot{q}_r]^T A_{21} [\ddot{q}_l(t - d_l) - A_{21} q_r] \\ &\quad - A_{22} \dot{q}_r + A_{21} q_r - q_r + A_{22} \dot{q}_r - \dot{q}_r - \ddot{q}_l(t - d_l) \\ &= [\dot{q}_l(t - d_l) - \dot{q}_r]^T A_{21} [\dot{q}_l(t - d_l) - \dot{q}_r] \end{aligned} \quad (7)$$

For  $A_{21} < 0$ ,  $\dot{V} < 0$  holds for all  $e_r \neq 0$  and  $\dot{e}_r \neq 0$ . Meanwhile,  $V \rightarrow \infty$  holds when  $e_r \rightarrow \infty$  and  $\|\dot{e}_r\| \rightarrow \infty$ . As a result,  $q_r$ ,  $\dot{q}_r$ ,  $e_r$  and  $\dot{e}_r$  are bounded, which implies stability of the system and position synchronization about the remote side are guaranteed. The proof is

Fig. 12. Prediction results about time delay  $dt_2$ .Fig. 13. Prediction errors about time delay  $dt_2$ .

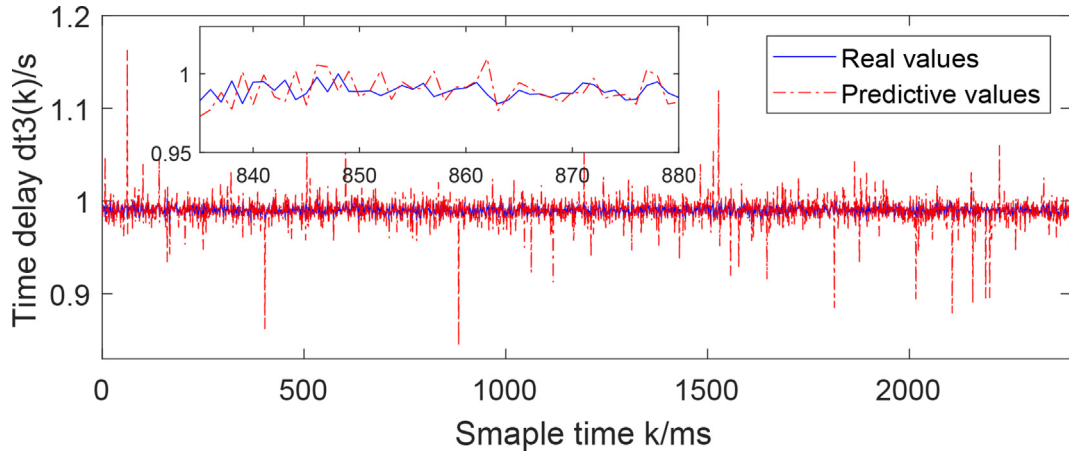
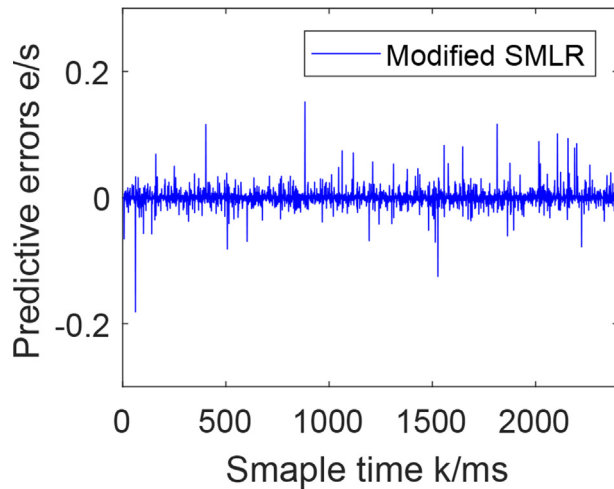
completed.

#### 4. Simulation

In this section, prediction results about  $dt_1$ ,  $dt_2$  and  $dt_3$  are given. Except for  $dt_1$ , real values of  $dt_2$  and  $dt_3$  are obtained from a low-orbit teleoperation experiment. Meanwhile, structure of the STS in our experiment is illustrated as Fig. 1. Actually, in practical STS, the measuring of time delay often is in the form of RTTD. But in this paper, to facilitate the comparison and illustration, RTTD is divided to three parts  $dt_1$ ,  $dt_2$  and  $dt_3$  in measurement. Then, four approaches (SMLR, modified SMLR, AR, NN) are utilized to realize the prediction of  $dt_1$ . Results

concerning prediction and prediction-error of  $dt_1$  are illustrated in Figs. 10 and 11, respectively. For  $dt_2$ , it changes in line with the cubic polynomial function varying rule. The CBMB (with least square parameter identification (LSPI)) and modified SMLR methods are adopted to forecast the  $dt_2$ . The prediction/prediction-error results for  $dt_2$  are given in Figs. 12/13. Finally, prediction/prediction-error results about  $dt_3$  with the modified SMLR method are given in Figs. 14/15.

According to Figs. 10 and 11, the modified SMLR shares more higher prediction precision comparing with AR and NN methods, especially when time delay exists huge jitters. Though prediction accuracy for the modified and traditional SMLR approaches is almost equal, the prediction efficiency of modified SMLR is far more than the

Fig. 14. Prediction results about time delay  $dt_3$ .Fig. 15. Prediction errors about time delay  $dt_3$ .

traditional SMLR method. Similarly, the modified SMLR behaves more well than the CBMB method in predicting  $dt_2$ , as the CBMB approach exists huge jitters in each switching point  $\frac{P_s}{4}$  during every revolution period  $P_s$ . For  $dt_3$ , the modified SMLR also shares good prediction capacity, as the average relative prediction is no more than 2.5%.

**Remark 3.** In this paper, all methods predict the time delay, online. Furthermore, almost all those approaches are with no off-line parameter identification. But there is also a special case, the AR approach have trained the parameters during the period 0–100 ms. This is because AR method share poor prediction property, if it is with no beforehand parameters training. For AR method in third subgraph of Fig. 10, the prediction haven't began during 0–100 ms. Moreover, in AR method, we use the real values to replace the prediction one during this period. Hence, it's not difficult to explain the good prediction results during 0–100 ms.

## 5. Conclusion

In this paper, time delay prediction for STS is studied. As Fig. 1 illustrated, time delay of STS is composed of three parts. Based on the elaborate varying rules and statistics analysis for different parts of time delay, a modified SMLR model method is proposed. The modified SMLR method can simultaneously predict all of those three parts of time delay. As time delay measurement is often in the form of RTTD, this ability of the proposed method is useful and helpful in space teleoperation. Especially, the modified SMLR behaves well when time delay

exists huge jumps and jitters, comparing with NN, AR and CPMB methods. Furthermore, the modified SMLR approach also shares high and stable prediction efficiency during the experiment. It is the main improvement comparing with the traditional SMLR illustrated in Ref. [30]. Obviously, it is very meaningful in space teleoperation for limited operation window time.

## Acknowledgement

This work was supported by the National Natural Science Foundation of China (Grant No. 61725303, 91848205).

## References

- [1] T. Imaida, Y. Yokokohji, T. Doi, M. Oda, T. Yoshikawa, Ground-space bilateral teleoperation of ETS-VII robot arm by direct bilateral coupling under 7-s time delay condition, *IEEE Trans. Robot. Autom.* 20 (3) (2004) 499–511.
- [2] J. Kofman, X.H. Wu, T.J. Luu, S. Verma, Teleoperation of a robot manipulator using a vision-based human robot interface, *IEEE Trans. Ind. Electron.* 52 (5) (2005) 1206–1219.
- [3] W.K. Yoon, T. Goshozono, H. Kawabe, M. Kinami, Y. Tsumaki, M. Uchiyama, M. Oda, T. Doi, Model-based space robot teleoperation of ETS-VII manipulator, *IEEE Trans. Robot. Autom.* 20 (3) (2004) 602–612.
- [4] T.J. Hu, X.X. Huang, Q. Tan, Time delay prediction for space teleoperation based on non-Gaussian auto-regressive model, *Proceedings of the 2012 IEEE International Conference on Robotics and Automation (ICRA 2012)*, 2012, pp. 567–572.
- [5] E. Nuño, L. Basañez, R. Ortega, Passivity-based control for bilateral teleoperation: a tutorial, *Automatica* 47 (2011) 485–495.
- [6] X. Xu, C. Schuwerk, B. Cizmeci, E. Steinbach, Energy prediction for teleoperation systems that combine the time domain passivity approach with perceptual dead-band-based haptic data reduction, *IEEE Trans. Hapt.* 9 (4) (2016) 560–573.
- [7] H.L. Wang, Passivity based synchronization for networked robotic systems with uncertain kinematics and dynamics, *Automatica* 49 (2013) 755–761.
- [8] A. Shahidi, S. Siroouspour, Adaptive/robust control for time-delay teleoperation, *IEEE Trans. Robot.* 25 (1) (2009) 196–205.
- [9] Y.N. Yang, C.C. Hua, X.P. Guan, Finite time control design for bilateral teleoperation system with position synchronization error constrained, *IEEE Trans. Cybern.* 46 (3) (2016) 609–619.
- [10] Y.N. Yang, C. Ge, H. Wang, X.Y. Li, C.C. Hua, Adaptive neural network based prescribed performance control for teleoperation system under input saturation, *J. Franklin Inst.* 352 (2015) 1850–1866.
- [11] Z.W. Wang, Z. Chen, B. Liang, B. Zhang, A novel adaptive finite time controller for bilateral teleoperation system, *Acta Astronaut.* 144 (2018) 263–270.
- [12] Z. Chen, Y.J. Pan, J.S. Gu, Adaptive robust control of bilateral teleoperation systems with unmeasurable environmental force and arbitrary time delays, *IET Control Theory Appl.* 8 (15) (2014) 1456–1464.
- [13] J.J. Zhang, W.D. Liu, L. Gao, L. Li, The master adaptive impedance control and slave adaptive neural network control in underwater manipulator uncertainty tele-operation, *Ocean Eng.* 165 (2018) 465–479.
- [14] Z.T. Chen, Z.J. Li, C.L. Philip Chen, Adaptive neural control of uncertain MIMO nonlinear systems with state and input constraints, *IEEE Trans. Neural Netw. Learn. Syst.* 28 (6) (2017) 1318–1330.
- [15] J.S. Farrokh, H. Iraj, Experimental analysis of mobile-robot teleoperation via shared impedance control, *IEEE Trans. Syst. Man Cybern.-Part B: Cybern.* 41 (2) (2011) 591–606.
- [16] I.S. Hyoung, T. Bhattacharjee, H. Hashimoto, Effect of impedance-shaping on perception of soft tissues in macro-micro teleoperation, *IEEE Trans. Ind. Electron.* 59

- (8) (2012) 3273–3285.
- [17] A.Y. Mersha, S. Stramigioli, R. Carloni, On bilateral teleoperation of aerial robots, *IEEE Trans. Robot.* 30 (1) (2014) 258–274.
- [18] C. Javier, S. Jorge, P. Angelika, Decision-making model for adaptive impedance control of teleoperation systems, *IEEE Trans. Hapt.* 10 (1) (2017) 5–16.
- [19] M. Sharifi, H. Salarieh, S. Behzadipour, M. Tavakoli, Impedance control of nonlinear multi-DOF teleoperation systems with time delay: absolute stability, *IET Control Theory Appl.* 12 (12) (2014) 1722–1729.
- [20] K. Yoshida, T. Namerikawa, Predictive PD control for teleoperation with communication time delay, *Proceedings of the 17th World Congress, The International Federation of Automatic Control*, 2008, pp. 12703–12708.
- [21] J.Q. Huang, F.L. Lewis, Neural-network predictive control for nonlinear dynamic systems with time-delay, *IEEE Trans. Neural Netw.* 14 (2) (2003) 377–389.
- [22] K. Yoshida, T. Namerikawa, Stability and tracking properties in predictive control with adaptation for bilateral teleoperation, *American Control Conference*, 2009, pp. 1323–1328.
- [23] T. Slama, D. Aubry, P. Vieyres, F. Kratz, Delayed generalized predictive control of bilateral teleoperation systems, *16th Triennial World Congress*, 2005, pp. 379–384.
- [24] S. Soroushpour, A. Shahidi, Model predictive control for transparent teleoperation under communication time delay, *IEEE Trans. Robot.* 22 (6) (2006) 1131–1145.
- [25] T. Slama, A. Trevisani, D. Aubry, R. Oboe, F. Kratz, Experimental analysis of an internet-based bilateral teleoperation system with motion and force scaling using a model predictive controller, *IEEE Trans. Ind. Electron.* 55 (9) (2008) 3290–3299.
- [26] Z.Y. Lu, P.F. Huang, Z.X. Liu, Predictive approach for sensorless bimanual teleoperation under random time delays with adaptive fuzzy control, *IEEE Trans. Ind. Electron.* 65 (3) (2018) 2439–2448.
- [27] P. Arcara, C. Melchiorri, Control schemes for teleoperation with time delay: a comparative study, *Robot. Auton. Syst.* 38 (1) (2002) 49–64.
- [28] R. Uddin, J. Ryu, Predictive control approaches for bilateral teleoperation, *Annu. Rev. Contr.* 42 (2016) 82–99.
- [29] H.J. Li, A.G. Song, Virtual-environment modeling and correction for force-reflecting teleoperation with time delay, *IEEE Trans. Ind. Electron.* 54 (2) (2007) 1227–1233.
- [30] D. Chen, X.H. Fu, W. Ding, H.Y. Li, N. Xi, Y.C. Wang, Shifted gamma distribution and long-range prediction of round trip time delay for internet-based teleoperation, *Proceedings of the 2008 IEEE International Conference on Robotics and Biomimetics*, 2009, pp. 21–26.
- [31] D. Chen, N. Xi, Y.C. Wang, H.Y. Li, X.S. Tang, Event-based predictive control strategy for teleoperation via internet, *IET Control Theory & Appl.* 27 (5) (2010) 359–364.
- [32] X.F. Ye, M.Q.H. Meng, P.X.P. Liu, G.B. Li, Statistical analysis and prediction of round trip delay for internet-based teleoperation, *IEEE/RSJ International Conference on Intelligent Robots and Systems*, 2002, pp. 2999–3004.
- [33] T. Mirfakhrai, S. Payandeh, A delay prediction approach for teleoperation over the internet, *IEEE International Conference on Robotics and Automation*, 2002, pp. 2178–2183.
- [34] F.P. Yang, X.Z. Wang, Y.H. Yang, H.Y. Li, Virtual system calibration based on jitter prediction of internet time-delay for teleoperation systems, *3rd IFAC International Conference on Intelligent Control and Automation Science*, 2013, pp. 497–502.
- [35] F. Yu, D. Chen, X.S. Tang, Time delay prediction method based on EMD and elman neural network, *6th International Conference on Intelligent Human-Machine Systems and Cybernetics*, 2014, pp. 368–371.
- [36] J.N. Hua, Y.J. Cui, Y.H. Yang, H.Y. Li, Analysis and prediction of jitter of internet one-way time-delay for teleoperation systems, *IEEE International Conference on Industrial Informatics*, 2013, pp. 612–617.
- [37] Y.H. Yang, H.Y. Li, Kernel based nonlinear regression for internet round trip time-delay prediction, *Proceedings of the 10th World Congress on Intelligent Control and Automation*, 2012, pp. 852–856.
- [38] R. Oboe, P. Fiorini, A design and control environment for internet-based tele-robotics, *Int. J. Robot. Res.* 17 (4) (1998) 433–449.
- [39] N. Emmanuel, O. Romeo, W.S. Mark, Position tracking for non-linear teleoperators with variable time delay, *Int. J. Robot. Res.* 28 (7) (2009) 895–910.